Combination of the Wenner resistivimeter and Torrent Permeameter methods for assessing carbonation depth and saturation level of concrete

Stéphanie BONNET[1], Jean-Paul BALAYSSAC[2]

[1] LUNAM Université, Université de Nantes, GeM, Institut de Recherche en Génie civil et Mécanique – CNRS UMR 6183 52 rue Michel Ange, BP 420, 44606 Saint-Nazaire cedex, France
stephanie.bonnet@univ-nantes.fr

[2] LMDC, INSA/UPS Génie Civil, 135 Avenue de Rangueil, 31077 Toulouse cedex 04 France
jean-paul.balayssac@insa-toulouse.fr

Abstract

Assessing carbonation depth is of great interest for the diagnosis of reinforced concrete structures because carbonation is one of the origins of steel corrosion. The assessment of carbonation depth is usually performed by a simple and reliable semi-destructive test consisting in spraying a colored indicator on a sample extracted from the structure. When the structure is large, this test must be reproduced many times if an assessment of the variability of carbonation depth is required. In this case, the extraction of multiple samples can be prohibitive from the technical and economic points of view. So, in this case, a non-destructive testing (NDT) method could be relevant. However, even when NDT methods can be used, there is a need to improve the interpretation of their results. In this study, the use of two usual NDT methods is proposed: resistivity measurement by a Wenner probe and surface permeability assessment by a Torrent permeameter. Both techniques are implemented on carbonated slabs having different carbonated depths and at different saturation degrees. The results show that the two techniques are sensitive to moisture and carbonation. For a given saturation level, resistivity increases when the carbonated depth increases and resistivity decreases when the saturation level increases. Torrent permeability decreases when the saturation degree and carbonated depth increase. Good repeatability is observed for resistivity measurements while a larger scatter is obtained for Torrent permeability. Empirical laws are

[1] Corresponding author. Tel.: +33 2 40 17 81 88;
E-mail address: stephanie.bonnet@univ-nantes.fr

built for the relationships between resistivity or permeability and saturation degree and carbonated depth. For resistivity, either a linear model between resistivity and saturation degree is used or Archie's law is adapted to take the effect of carbonation into account. Following the same idea, a linear law between Torrent permeability and saturation degree is adapted to the effect of carbonation. Because resistivity can be measured only if the saturation degree is rather high, i.e. if there is a continuity of the interstitial solution, and because permeability assessment is impossible if the concrete is fully saturated, these laws are limited to saturation degrees in the 40 to 83% range.

Then, these laws are used to predict carbonation depth and saturation degree on a wall designed with the same concrete but stored in different conditions. The results show that resistivity and Torrent permeability can be used for the combined assessment of carbonation depth and saturation degree in laboratory conditions.

Keywords: Concrete, carbonation depth, saturation level, Torrent permeability, Wenner resistivity

1 Introduction

The corrosion of reinforcing steel within reinforced concrete structures produces damage such as spalling of the concrete cover. Steel parts then remain uncovered and cause a sharp decrease in the load-bearing capacity of the structure. This failure condition is usually due to the presence of chloride or to a carbonation process. The present study was conducted to examine, more specifically, the carbonation process. Carbonation is a physical-chemical process, which may cause a decrease in concrete pH value from 13 to 9. Carbon dioxide from the air (CO_2) reacts with the portlandite of concrete ($Ca(OH)_2$) to form calcium carbonate ($CaCO_3 + H_2O$) (Figure 1). If the whole of the concrete cover is carbonated, steel frame de-

passivation is initiated and results in the delamination of the concrete cover due to swelling of the corroded steel.

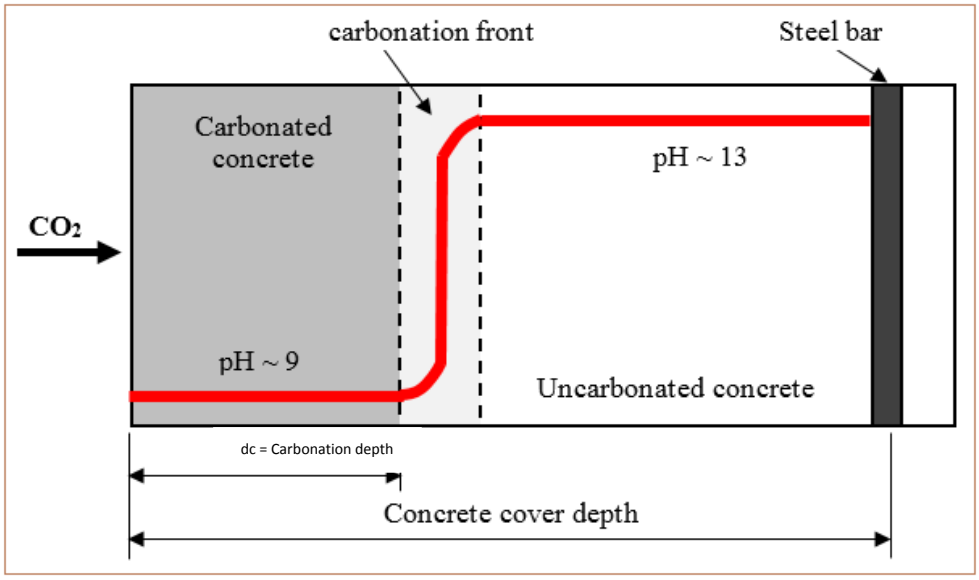

Figure 1: pH decrease in concrete cover due to carbonation [Ta 2016]

According to a literature review conducted by Ta et al. [Ta 2016 and 2018], a considerable amount of effort has been devoted to the study of the propagation of CO_2 and to the examination of the factors affecting the carbonation rate, such as mix proportions in concrete (e.g., cement content and water to cement ratio) [Chang 2004], [Papadakis 1989], mineral admixtures [Hui-Sheng 2009] [Papadakis, 1999 and 2000] [Younsi 2011], exposure conditions (e.g., temperature (T) [Saetta 1993] and external relative humidity (RH) [Houst 1983] [Papadakis, 1989]).

Because carbonation takes place throughout the life cycle of concrete, accurate assessment of its progress is essential to predict the initiation of steel corrosion. To achieve this, the condition of the concrete cover of structures must be surveyed at regular intervals in order to plan maintenance. The most common technique used for measuring carbonation depth is the semi-destructive coring method [RILEM CPC-18]. Phenolphthalein is sprayed on the fresh cores obtained [Chang 2006, Villain 2006]. Phenolphthalein is an organic compound used as a

pH indicator: it is colorless at low pH values (around pH 9) but has a characteristic purple or magenta color at pH values exceeding 10.5.

Testing is carried out at structure level with a sufficiently representative number of measurement points, requiring a large variety of core samples [Breysse, 2017]. For improved conservation of structures, non-destructive survey techniques must be favored as they can be used to detect and characterize defects or damage without the need for coring [Bungey 2006].

The objective of this research is to examine the sensitivity to the presence of carbonation in concrete structures of two currently available non-destructive methods: the Torrent permeameter and the Wenner resistivimeter. Carbonation affects the microstructure of concrete by reducing porosity [Nagla 1997, Auroy 2015] because the volume of hydrates increases by an average of 11.7% [Song and Kwon 2007]. As the carbonation front progresses, an increasing number of pores become clogged and reduce porosity in the depth of carbonated concrete. Porosity is one factor among others (e.g. water content and rebars) affecting resistivity measurements in cementitious materials. Sbartaï et al. [Sbartaï 2007] have demonstrated that resistivity increases when the W/C ratio of the studied concrete decreases, leading to decreased porosity. A similar trend was observed by Lübeck et al. [Lübeck 2012] after measuring concrete specimens with different water to binder ratios. As regards permeability, some studies addressing the problem of permeability measurements using the Cembureau method have shown that permeability decreases with the porosity of the studied concrete [Hui-Sheng 2009] [Djerbi 2008 and 2013]. This trend is also reflected by permeability measurements performed using the Torrent permeameter: Romer has measured greater permeability values in mortars with a W/C ratio of 0.6 than in mortars with a W/C ratio of 0.35 [Romer 2005] and the same tendency was also found by Neves et al. [Neves 2012]. The results presented by Neves et al. show that the permeability values obtained using the Torrent method decrease as compressive strength rises and that porosity therefore

decreases [Neves 2015]. Sena da Fonseca et al. found a relation between Torrent air-permeability and open porosity measured on stones [Sena da Fonseca 2015]. So it can be assumed that the permeability of carbonated concrete is bound to decrease and that, conversely, its resistivity may increase. We therefore selected two already available non-destructive methods: the Wenner resistivimeter [Polder 2001] used to measure concrete resistivity and the Torrent permeameter [Torrent, 1992] used to measure surface permeability.

In situ measurements were carried out on structures that were never completely dry for auscultation. Depending on the weather conditions, the saturation degree of concrete may differ. Because resistivity and permeability are both sensitive to concrete moisture content, the sensitivity must be taken into account in the measurement analysis of both devices. The influence of the resistivity as a function of the saturation level has been investigated by Sbartaï et al. [Sbartaï 2007] and the results demonstrate that concrete electrical resistivity decreases when saturation level increases. Resistivity varies between 54 and 960 Ω.m but cannot be measured when the saturation level is less than 60%. Similar results are found in other studies. In [Saleem 1996], resistivity ranges from 80 to 780 Ω.m and, the lower the water content, the higher the resistivity. At a mass water content of about 1.5%, the resistivity cannot be measured because the concrete slab is too dry to allow the current to flow within the sample. The work of Lopez and Gonzalez [Lopez and Gonzalez, 1993] underlines the effect of the pore saturation level in relation to resistivity. They carried out tests on mortars with a W/C ratio of 0.5. The resistivity values changed within a narrow range when the pore saturation level varied between 60 and 100%. Then, between 60 and 30%, the resistivity increased sharply, up to a limit corresponding to a saturation level at which measurement was impossible. Recent studies have improved the resistivity techniques to monitor water and chloride ingress in concrete by using a multi electrode resistivity system [Du Ploy 2015, Lecieux 2015, Fares 2018].

Gas permeability is a transport property characterizing gas flow under a pressure gradient and is used to determine the speed with which a gas (potentially an aggressive gas like carbon dioxide) may penetrate into concrete. Air permeability is affected by the concrete moisture content and the concrete saturation level has been shown to have an effect on transport properties. For instance, the air permeability of a concrete specimen, measured using the Cembureau method, increases when the saturation level decreases [Villain 2001, Picandet 2001]. Kameche et al. [Kameche 2014] confirmed this influence and the present study was conducted to examine the intrinsic permeability variations of CEM II concrete materials according to the degree of saturation, from a saturated state to a completely dry state. Because gas intrinsic permeability decreases when the saturation level increases, Cembureau measurements are not possible with saturation rates above 80%. Romer conducted an experimental study to assess the Torrent and Cembureau methods in CEM I mortar samples prepared with different cement contents [Romer, 2005]. The tests were carried out by varying the relative humidity of the samples via processing at different ambient conditions. The results thus obtained confirm that the permeability values measured using both Cembureau and Torrent methods increase as the samples become drier. However, the study does not determine the sample saturation level.

It thus appears from the studies listed above that both resistivity and permeability decrease when the saturation level increases. Moreover, resistivity measurements are possible with saturation rates above 30% (water content higher than 1.5%) whereas Cembureau permeability measurements are only possible with rates below 80%.

Permeability is a transport property depending on the porosity of the material studied. Because carbonation decreases porosity, the surface permeability of carbonated concrete measured using the Torrent permeameter can be expected to change. As regards water permeability, the water flow is weaker in carbonated than in non-carbonated concrete [Song

and Kwon, 2007]. Auroy et al. underline a decrease in intrinsic permeability after carbonation for CEM I Portland cement [Auroy, 2015].

Similarly, because resistivity is affected by the material microstructure, variations in resistivity can be expected according to the carbonation depth. However, the literature reviewed for this paper contains no research on the resistivity and permeability of carbonated concrete specimens using Wenner's and Torrent's methods. The present study, therefore, addresses carbonation and moisture effects on resistivity and permeability measurements in terms of both quality and quantity in laboratory conditions. It is also important to note that rebar close to surface affects the resistivity. We chose to avoid this effect as it is difficult to evaluate, except maybe by using a numerical model for the determination of apparent resistivity [Nguyen 2017].

Using the Wenner resistivimeter and the Torrent permeameter, and taking account of the sensitivity of the measurement equipment, resistivity and permeability results measured in concrete slabs made of the same mixture, with varying carbonation depths and saturation levels ranging from a dry state to a saturated state, were determined. The experimental results are analyzed below and translated into laws considering the dispersion of the measurement values. The objective of this analysis is the simultaneous use of both non-destructive methods (NDT) to assess saturation level and carbonation depth in real structures. Finally, the laws of correlation established were validated using a concrete wall made of the same concrete mix as the experimental slabs.

2 Materials and experimental program

2.1 Concrete specimens

The concrete mix was composed of CPA-CEM I 52.5 Portland cement with a water/cement ratio of 0.8 to accelerate the carbonation process (Table 1). Eleven slabs (rectangles 50 x 25 and 12 cm thick) were prepared from a single batch of concrete in a laboratory in Toulouse (France): nine were cast for non-destructive testing, one was used for determining the physical and mechanical properties and the last one was sealed on five faces and put into the carbonation chamber to monitor carbonation depth. The concrete mixtures were cast in plastic molds and compacted under vibration. After casting, the slabs were stored in a room at 20 °C with about 95% relative humidity (RH) for 24 h until demolding, after which they were cured in water at 20 °C for 28 days.

After 28 days, two slabs were used to assess the mechanical and physical properties of the concrete. Cylindrical cores were extracted from these slabs to drive these tests. The results are summarized in Tables 2 and 3. Open porosity was measured using the water saturation method on three specimens. Three specimens were tested under axial compressive loading conditions with measurement of lateral and axial displacements, and three other discs were sealed with two layers of adhesive aluminum tape to ensure a one-dimensional gas flow through the discs. These specimens were oven-dried at 105 °C to constant weight before permeability testing was conducted using the Cembureau device.

Constituents (kg/m3)	**OPC C1**
Cement CEM I 52.5 N CE CP2 NF	240
Siliceous Sand 0/2 or 0/4	941
Siliceous aggregates 4-14 or 10-14	1019
Water	193
Superplasticizer	0.96
W/C	0.8
Slump (cm)	14

Table 1: Mix proportions of concrete

Properties	OPC C1
Dry apparent density (kg/m^3)	2 222
Open porosity measured by water saturation method (%)	18.3
Cembureau apparent permeability with an injection pressure of 0.5 bars measured in dried specimen (10^{-16} m²) (= K_{ref},C)	7.71

Table 2: Physical and transport properties (average of three measurements)

Mechanical properties (28 days)	OPC C1
compressive strength (MPa)	21.5
Modulus of elasticity (MPa)	24927
Poisson ratio	0.208

Table 3: Mechanical properties at 28 days (average of three measurements)

2.2 Carbonation procedure

The nine slabs intended for non-destructive testing were referenced as N or T (Table 4). After exposure to carbonation, the slabs referenced N were stored in Nantes (France) and those referenced T, in Toulouse.

After a 28-day residence time in water, the slabs were oven-dried at 80 °C until constant weight was reached. The dry mass, $W_{d,}$ was used to calculate the water content at time t (Equation 1), which, in turn, was used to calculate the degree of saturation at time t (Equation 2). At the end of the drying phase, the slabs were stored in laboratory conditions. The four slabs referenced as 1 (C1-1-7N, C1-1-8N, C1-1-1T, C1-1-2T) were completely sealed with two layers of adhesive aluminum tape to prevent carbonation. The slabs referenced C1-2N, C1-3N, C1 4N, C1-2T, and C1-3T were sealed on five faces only, to ensure a one-dimensional carbonation processing from one side of the slab only (50 cm x 25 cm). These slabs were placed in a chamber at 20 °C, with a relative humidity of 65% and a CO_2 content of 50% to accelerate the carbonation process. The core samples were extracted from the

specific sampling slab at the end of the curing phase and stored with the slabs in the laboratory. They were also placed in the carbonation chamber to monitor carbonation progress, just like the slabs. However, during this phase, the different core samples were regularly broken and immediately sprayed with the phenolphthalein color indicator so as to assess the carbonation depth at a given point of time. When the different desired carbonation depths had been reached on the control core samples, the slabs were removed from the chamber and immersed in water to stop carbonation and to ensure complete saturation of the slabs.

The real carbonation depths measured after completion of the whole experimental procedure using NDT techniques, are presented in Table 4.

Slab reference	**Expected carbonation depth (mm)**	**Measured carbonation depth d_c (mm) (cf. Figure 1)**
C1-1-7N	0	0
C1-1-8N	0	0
C1-2N	10	9.1
C1-3N	20	18.2
C1-4N	30	27.3
C1-1-1T	0	0
C1-1-2T	0	0
C1-2T	10	10.5
C1-3T	20	17

Table 4: Expected and measured carbonation depths

2.3 Experimental procedure

The operating method consisted in varying the slab water content in order to obtain permeability and resistivity correlation curves according to the saturation level. After saturation, different phases of drying were undertaken in order to achieve measurements with

targeted water contents corresponding to identical saturation levels for all the slabs. For that purpose, the slabs were placed in a drying oven at 80 °C and dried while their weight loss was monitored. It was assumed that the concrete was not modified at 80 °C, since ettringite is considered to dehydrate at a temperature higher than 80 °C [Zhou and Glasser 2001] and therefore would have remained almost stable at 80 °C. When the targeted mass was obtained and the drying phase completed, the slabs were hermetically sealed in airtight bags for forty days to balance the humidity level of the slabs and prevent natural carbonation. Their mass was measured regularly to leak-check the bags. Once the slabs were taken to be homogenized, the slab mass, W(t), was measured again. Then, resistivity and permeability measurements were carried out. The water content was determined from Equation 1:

$$w(t) = (W(t)-W_d)/W_d \quad (1)$$

where w(t) is the water content at time t, W(t) is the mass of the slab at time t (kg) and W_d is the mass of the dried slab (kg).

The degree of saturation at time t is obtained from Equation 2 as:

$$S(t) = w(t)/ w_{sat} \quad (2)$$

where w_{sat} is the water content of the saturated slabs.

For each measurement method (Wenner resistivimeter and Torrent permeameter), a total of ten measurements per test point and saturation level were performed. Measurements were carried out in the center of all the slabs (Point 1 in Figure 2). However, in order to check slab homogeneity and measurement sensitivity to side effects, measurements were also carried out on either side of Slab C1-1-8-N center (Points 2 and 2' in Figure 2). The measurements were made first at point 1, then at point 2 and finally at point 2' before returning to spot 1. So there was enough time between consecutive measurements in the same spot to allow vacuum dissipation.

The Wenner resistivity measurements were first carried out to determine the resistivity values, which were afterwards used for the Torrent surface permeability measurements [Torrent 1992].

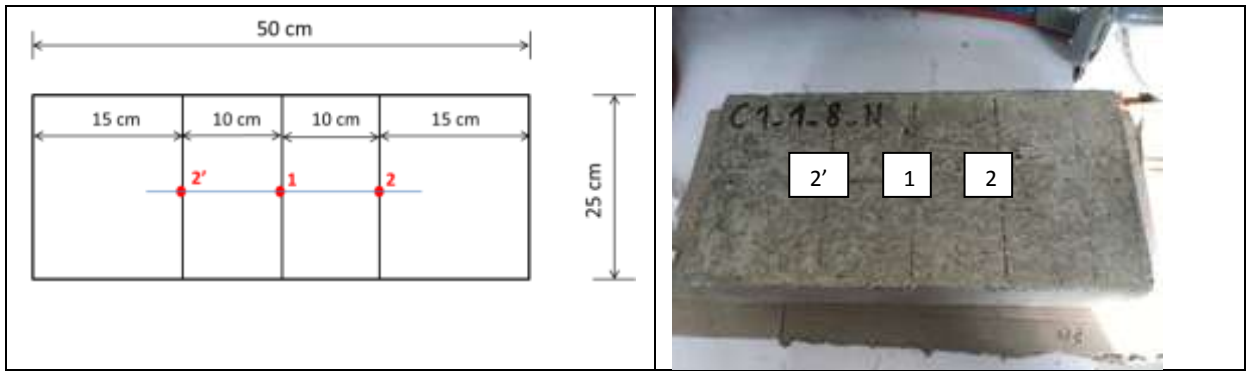

Figure 2: Location of measurement points on the slabs

The Wenner resistivimeter is a measurement device using Wenner protocol to determine the apparent resistivity of concrete facings. Measurements are assumed to be carried out on a semi-infinite homogeneous material. The measurement device is called a Wenner resistivimeter because of the electrode arrangement, in which the distance interval between the electrodes, called a, is the same, with a= $\overline{C_1P_1} = \overline{P_1P_2} = \overline{P_2C_2}$ (Figure 3). The device used in this work had a distance interval of 5 cm. First, an electric current, I, is injected between electrodes C1 and C2. Then, the electrical potential is measured between electrodes P1 and P2. The apparent resistivity is calculated by the control acquisition unit, based on the following formula:

$$\rho = 2\,\pi\,a\frac{V}{I} \qquad (3)$$

where ρ is the resistivity in Ω.m, a is the distance interval between the electrodes in m, V is the voltage in volts and I is the current intensity injected into the sample in amperes.

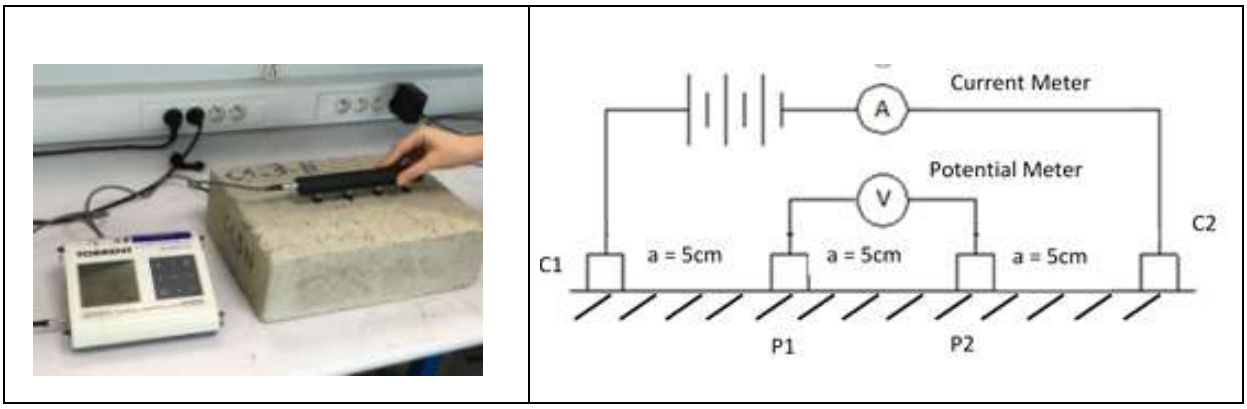

Figure 3: Wenner resistivity measurements

After the resistivity measurement was finished, the Torrent permeability was measured, if possible, depending on the slab saturation level. The test principle is to create a vacuum inside the test chamber using a vacuum pump and then disconnect the pump when the desired pressure is reached (Figure 4).

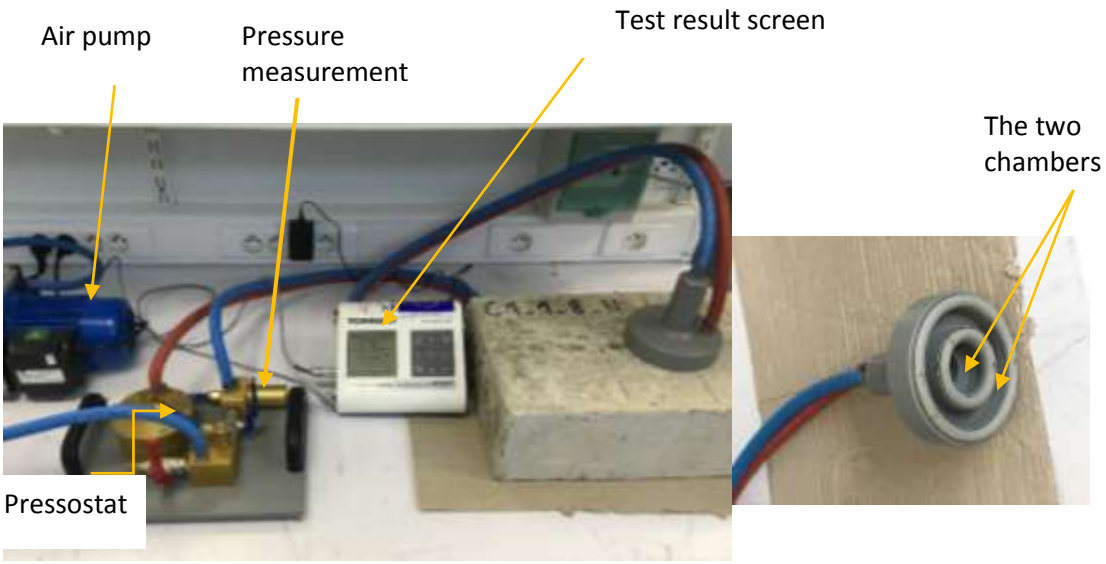

Figure 4: Torrent permeameter

The rate of increase of pressure inside the vacuum cell can be measured and the air permeability can be calculated according to the following formula:

$$K = \left(\frac{V_c}{A}\right)^2 . \frac{\mu}{2\,\varepsilon\,P_a}\left[\frac{\ln\left(\frac{P_a+\Delta P}{P_a-\Delta P}\right)}{\sqrt{t}-\sqrt{t_0}}\right]^2 \qquad (4)$$

300 with: K: Torrent gas permeability coefficient (m^2),

301 μ: Air dynamic viscosity at 20 °C (2.0.10-5 N.s/m^2),

302 Vc: Capacity of the inner chamber and of the elements, through which air flows during

303 the filling phase (Vc = 222.10^{-6} m^3),

304 ε: Concrete porosity introduced in the data (18.3 %, cf. Table 2).

305 A: concrete cross-section where air flows in the vacuum cell ($19.6.10^{-4}$ m^2),

306 ΔP: Pressure difference in the inner chamber in N/m^2,

307 Pa: Atmospheric pressure in N/m^2,

308 t0: Test start time (60 s),

309 t: Test duration (< 720 s).

310

311 # 3 Results

312 ## 3.1 Resistivity results

313 Resistivity measurements at the three points on a given slab showed little scatter in the results,
314 indicating that the concrete was homogeneous over the whole slab volume. It was concluded
315 that the saturation level of the slab was spatially homogeneous on the surface investigated.
316 Moreover, resistivity values were not influenced by side effects. Consequently, only the
317 average of the different measuring points appears in Figures 5 to 8. The standard deviations
318 were calculated from thirty measurements (ten measurements for Point 1, ten measurements
319 for Point 2 and ten measurements for Point 2').

320 For saturation levels below 41%, measurements proved impossible for the most carbonated
321 slab because it was too dry to allow electricity to flow freely between the electrodes.

322 Whatever the carbonation depth reached, Figure 5, 6, 7 and 8 show a lower resistivity when
323 the sample saturation level increases. The trend observed in Figures 6 and 7 for non-
324 carbonated samples has been highlighted by many authors [Sbartaï 2007, Saleem 1996, Lopez

1993]. When the saturation level decreases, the concrete liquid phase gradually changes to a discontinuous pattern that makes ion conduction more difficult. Resistivity values then increase sharply. In non-carbonated slabs, resistivity increases by a factor of six between saturated samples and samples with a 41% saturation level. This explains the non-linear behavior of the electrical resistivity in relation to the variations of concrete saturation levels.

Carbonation depth also affects resistivity. For the same saturation level, resistivity increases because of concrete structural changes due to carbonation reactions. The decrease in porosity induced by carbonation increases the material compactness, resulting in a less prevalent liquid phase. The current then flows less freely and resistivity increases.

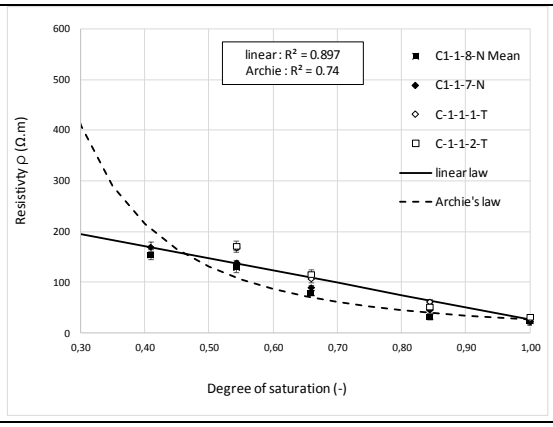

Figure 5: Resistivity versus saturation degree for non-carbonated slabs

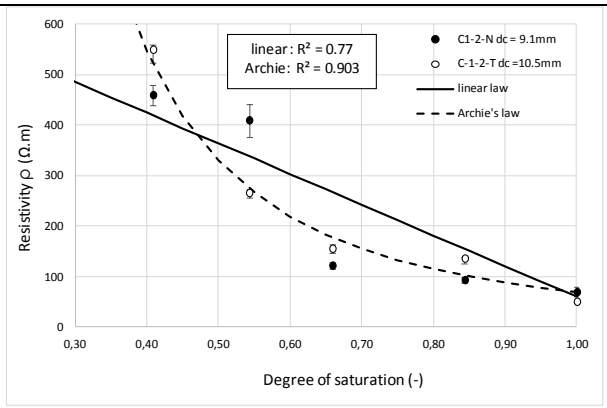

Figure 6: Resistivity versus saturation degree for carbonated slabs C1-2-N and C1-2-T (d_{cmean}= 9.8 mm)

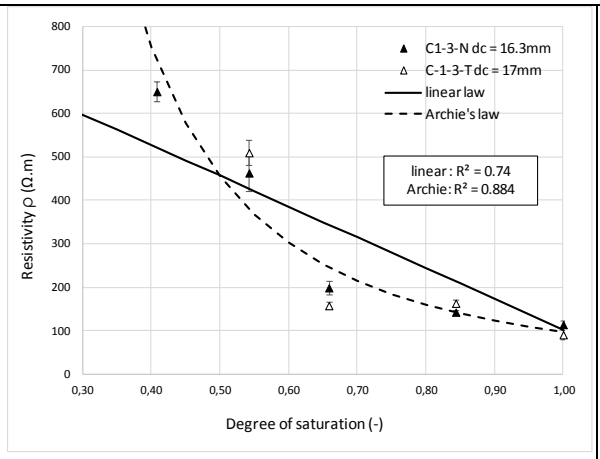

Figure 7: Resistivity versus saturation

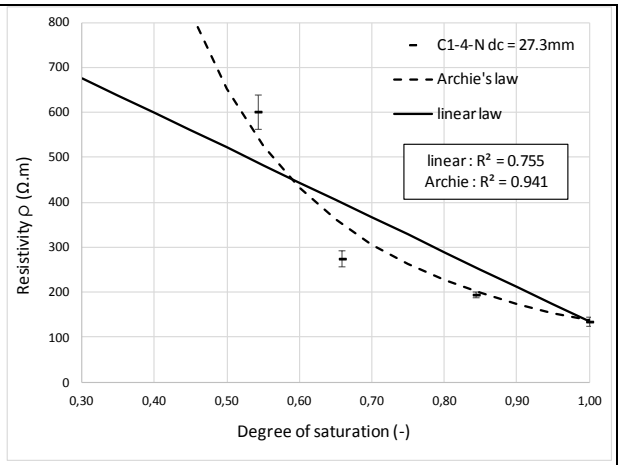

Figure 8: Resistivity versus saturation degree

degree for carbonated slabs C1-3-N and C1-3-T (d_{cmean}= 16.65 mm)	*for carbonated slab C1-4-N with d_c= 27.3 mm*

Some mathematical laws are now examined for best fitting of the experimental points. We first select a linear law because the results achieved for the non-carbonated slabs, within the saturation level range for which measurements are possible, follow a linear trend. Then the linear equation to determine the mean resistivity of saturated slabs when the degree of saturation is 100% is taken as:

$$\rho = a * (1 - S) + b \quad (5)$$

In the case of non-carbonated and fully saturated slabs, b is the reference value ρ_{ref}, called the reference resistivity. This value corresponds to the mean resistivity obtained on non-carbonated slabs in saturated conditions (C1-1-8-N, C1-1-7N, C1-1-1-T, C1-1-2-T). Here, the value of b is 27.627 Ω.m.

In the case of carbonated slabs, b is the mean resistivity calculated from the two saturated slabs (S=100%). For a carbonation depth of 27.3 mm, the value of b is obtained using Slab C1-4-N only. The values of a obtained by fitting the experimental data using Equation 5 are reported in Table 6.

The empirical Archie's law [Archie 1942] is also used to describe the general trend identified in these figures. This law describes the dependency of resistivity on the degree of saturation (S), porosity (ϕ) and resistivity of the composition pore solution (ρ_{sol}) as:

$$\rho = \rho_{sol} * S^{-n} \phi^{-m} \quad (6)$$

Parameters m and n are usually regressed over the experimental data.

To use this law, some parameters must be set. The pore solution resistivity is assumed to be constant throughout the carbonation process. However, it is reasonable to believe that the

change in the cement matrix due to the dissolution of the portlandite modifies the pore solution and therefore its conductivity.

The conductivity of the pore solution ($\sigma sol=1/\rho_{sol}$) can be expressed as:

$$\sigma_{sol} = \sigma_{wat} + \Sigma(C_i * \lambda_i) \quad (7)$$

where $\sigma_{wat} = 10^{-5}$ S/m , corresponding to the water conductivity as found in [Shi 2003]

C_i ionic content (mol/m3)

λ_i ionic molar conductivity (S.m²/mol)

The conductivity of the pore solution is assessed by combining data by Andersson et al. [Andersson 1989] and Nguyen [2006] (Table 5). Two solution conductivities are calculated: σsol = 8.92 S/m with the values by Nguyen and σsol = 6.41 S/m with the values by Andersson. Both these authors used very similar Portland cement but the mixes were different. The mean value (σ_{sol} = 7.66 S/m) is used to calculate the resistivity of the pore solution of the sample tested. This value is of the same order of magnitude as the values found in the literature, although the literature values obviously depend on cement type and water to cement ratios [Sanish 2013, Sant 2011, Neithalath 2006].

Ion	Ionic molar conductivity (mS.m²/mol)	Ionic content (mol/m^3) [Nguyen 2006]	Ionic content (mol/m^3) [Andersson 1989]
Na^+	5,01	100	42.3
K^+	7.35	272	161.1
Ca^{2+}	11.9	2.6	2.2
Cl^-	7.63	0.5	Not evaluated
OH^-	19.86	321.4	251.2 (calculated using measured pH)

Table 5: Values used to calculate the conductivity of the pore solution

In order to determine the factor n, which is assumed to be constant for both carbonated and non-carbonated slabs, the data obtained on non-carbonated slabs are used. In this case, the factor m is calculated using Archie's law for S=100% ($\rho_{ref} = \rho_{sol} * \phi^{-m_{ref}}$). We then have m_{ref} = 3.153 with ρ_{ref} =27.627 Ω.m. The factor n is therefore determined by fitting the experimental data of the non-carbonated slabs using Archie's law as: n = 2.24 (Figure 5). For the carbonated slabs (Figures 6, 7 and 8), n is kept constant and only m is adjusted to achieve the best possible fitting with the experimental data because it is assumed to depend on the microstructure, which changes during carbonation.

Table 6 displays the different law parameters and determination coefficients obtained. Both laws can be used to represent the trend obtained because the determination coefficients are correct in both cases. The determination coefficients given by the linear law, however, are lower, except on non-carbonated slabs, as the linear law does not represent points obtained for low saturation levels very accurately. It seems likely that, for a dry material, resistivity tends toward a very high value. This trend is thus best represented by Archie's law.

		a/n	b/m	Determination coefficient R^2
Non-carbonated slabs	Linear	238.16	27.627	0.897
	Archie	2.24	3.153	0.74
$d_{c\ mean}$ = 9.8 mm	Linear	725.955	59.9	0.77
	Archie	2.24	3.70	0.903
$d_{c\ mean}$ = 16.65 mm	Linear	864.852	102.63	0.74
	Archie	2.24	3,89	0.884
d_c = 27.3 mm	Linear	913.16	135	0.755
	Archie	2.24	4.10	0.941

Table 6: a and b (linear law), n and m (Archie's law) and corresponding determination coefficient R^2

The relations of coefficients a and b with mean carbonation depth are described as a logarithmic function (Equation 8) with R^2 = 0.984 and a linear function (Equation 9) with R^2

= 0.982, respectively. As regards Archie's law, the plot of coefficient m versus mean carbonation depth is described by a linear function with $R^2 = 0.91$ (Equation 10).

$$a = 91.645 * \ln(d_c) + 442.03 \quad (8)$$

$$b = 4.0198 * d_c + 27.627 \quad (9)$$

$$m = 0.0389 * d_c + 3.153 \quad (10)$$

By combining relationships 5 and 6 with Equations 8, 9 and 10, we obtain the laws describing electrical resistivity versus carbonation depth and saturation degree, respectively (Equations 11 and 12):

$$\rho = (91.645 * \ln(d_c) + 442.03) * (1 - S) + (4.0198 * d_c + 27.627) \quad (11)$$

$$\rho = \rho_{sol} * S^{-2.24} \phi^{-(0.0389 * d_c + 3.153)} \quad (12)$$

where d_c is the carbonation depth in mm and ρ the Wenner resistivity (Ω.m)

The coefficients of determination obtained for the linear law parameters are higher than that obtained for parameter m of Archie's law. These laws may be used for the calculation of the saturation level from a resistivity measurement with knowledge of the carbonation depth. This depth would have been determined, for instance, by spraying phenolphthalein on a freshly drilled core sampled from the structure. Carbonation depth determination is faster than saturation level determination because it can be read immediately after sampling without waiting for the complete drying needed for saturation level measurements. However, the laws established here apply only to concrete with similar porosity (about 18%) and mixed with CEM I cement. Solution resistivity and carbonation process both depend on the type of cement and any addition modifies the chemical reactions. These laws should also consider the measurement error aspects. In order to seriously take the standard deviations displayed in Figures 5, 6, 7 and 8 into account, Figure 9 presents the Coefficient of Variation (CoV),

corresponding to the standard deviation divided by the average of the values measured, for all the saturation levels. CoV values are very low (lower than 10% when the value obtained from the saturation measurements carried out on the non-carbonated slabs is eliminated). Moreover, this maximum value of 20% is of the same order of magnitude as the CoV calculated from laboratory measurements (approximately 18%) [Aït-Mokhtar, 2013]. It may be recalled that measurements appear reliable here, because the lower the CoV value, the higher the measurement accuracy. The results obtained on the non-carbonated slabs correspond to the lowest resistivity values and, hence, to higher CoV values. This analysis suggests that the Wenner measurements carried out using this device can be reproduced.

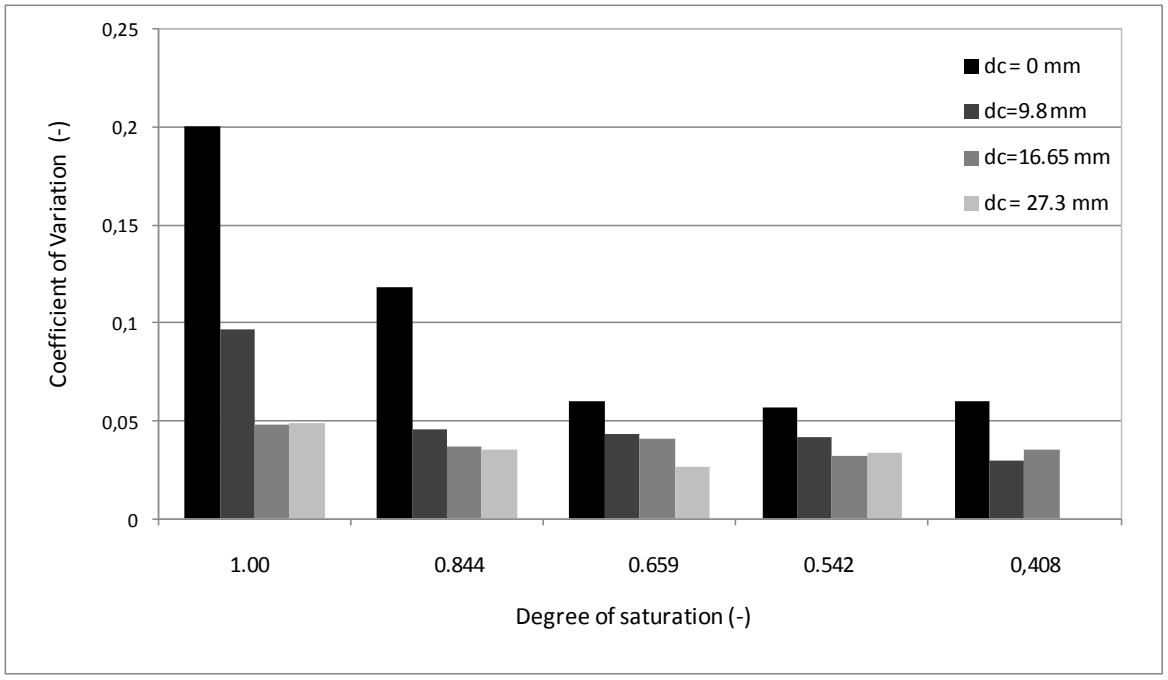

Figure 9: Coefficient of variation of the resistivity measurements as a function of saturation degree and carbonation depth

3.2 Air permeability results

Permeability measurements at the three points on a given slab showed scatter in the results. The differences observed cannot be attributed to the heterogeneity of the concrete material as all the resistivity measurements performed on the same slab for a given saturation level are

almost identical whatever the measurement point. Because side effects have not been demonstrated, the three point averages are presented with, on either side, the range defined by the standard deviation calculated from all the values (30 measurements). Moreover, on different concrete compositions, Neves et al. showed that, if the average of a set is used as the representative value, it is possible to distinguish between different concrete mixes and different curing (for the same mix) [Neves 2012].

Figures 10 through 13 show that, for a given carbonation depth, gas permeability decreases when the saturation level increases and also decreases when carbonation depth increases. Permeability also varies greatly in the slabs, which are supposed to be of the same concrete and in the same saturation state. Figure 10 shows that, when Sr = 15%, permeability ranges from 17 to 25.10-16 m², i.e. an increase of almost 50%. Although measurements are not possible on the fully saturated samples, they can, nevertheless, be performed up to 84%. Above this saturation rate, gas can no longer flow freely because of water molecule continuity in the concrete porous network. Concrete relative humidity reduces pore interconnectivity and, therefore, affects its permeability. The permeability vs. saturation level curve has already been assessed in the literature for non-carbonated materials using Cembureau measurements carried out on different concrete types [Kameche 2014, Abbas 1999]. These authors have established a logarithmic law to describe, as far as possible, the experimental results regarding intrinsic permeability as a function of saturation level for different sample sizes. Measurements are possible up to approximately 80% of the saturation level. As regards the work of Abbas et al. [Abbas 1999], a linear law best represents the results obtained for the apparent permeability measurements at different pressures as a function of the saturation level, with a saturation threshold of 90%. It should, however, be noted that the measurement variation ranges of both studies are larger than that obtained in the present paper using the Torrent permeameter, which results in a logarithmic display of their results. The present

results, on the other hand, are displayed on a linear scale for viewing comfort. They are fitted with a linear law for all the carbonation depths reached by imposing zero permeability as a condition for the saturated samples (S = 100%). This law is described by Equation 13. As regards dry, non-carbonated slabs, the reference value, $K_{ref,T}$ is imposed as the value for a. This value corresponds to the average obtained from the Torrent permeability measurements carried out on the dry non-carbonated Slabs C1-1-8-N, C1-1-7-N, C1-1-1-T and C1-1-2-T, is 27.34 10-16 m².

$$K = a * (1 - S) \quad (13)$$

The coefficients of determination are correct in view of the large standard deviations, which make it possible to confirm that the linear laws express Torrent permeability evolution satisfactorily as a function of the saturation level.

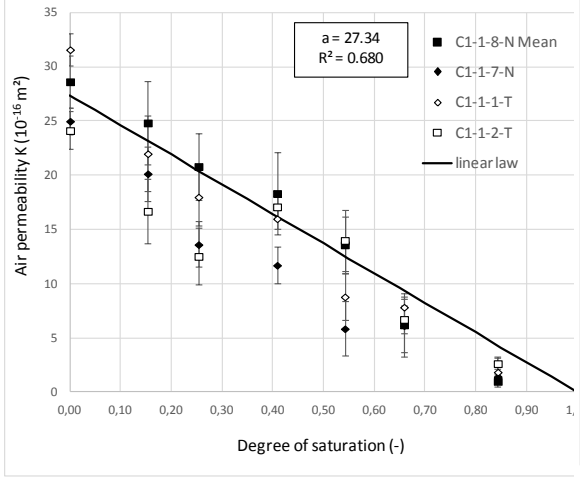

Figure 10: Torrent permeability versus saturation level for non-carbonated slabs

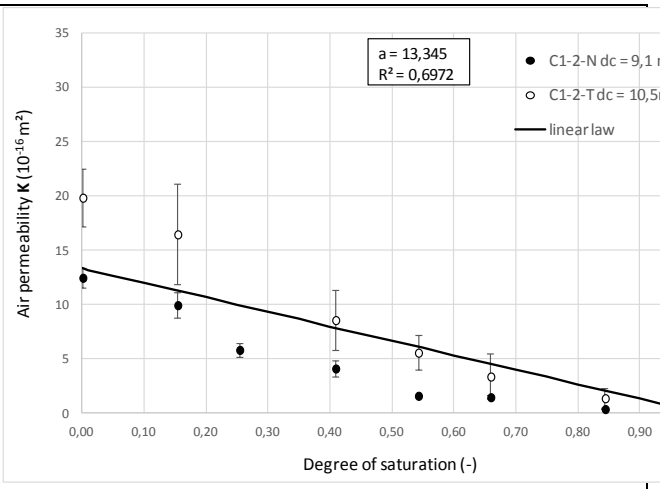

Figure 11: Torrent permeability versus saturation level for carbonated slabs C1-2-N et C1-2-T ($d_{c\ mean}$ = 9.8 mm)

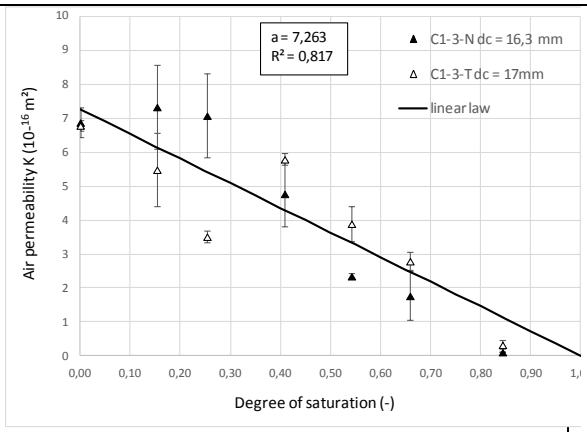

Figure 12: Torrent permeability versus saturation level for carbonated slabs C1-3-N et C1-3-T (d_{cmean}= 16.65 mm)

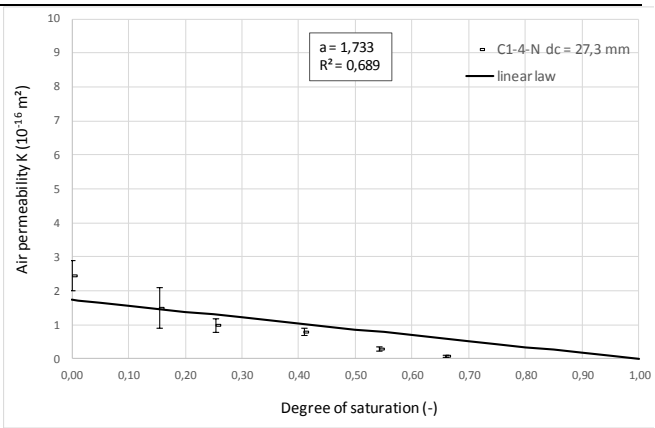

Figure 13: Torrent permeability versus saturation level for carbonated slabs C1-4-N (d_c = 27.3 mm)

Equation 14 describes coefficient a versus carbonation depth and is then introduced into Equation 15 to obtain Torrent permeability as a function of carbonation depth and saturation degree. Law 14 is obtained with a good determination coefficient $R^2 = 0.964$. Both equations take the form:

$$a = 27.34 * e^{-0.0935 * d_c} \quad (14)$$

$$K = (27.34 * e^{-0.0935 * d_c}) * (1 - S) \quad (15)$$

where d_c is the carbonation depth in mm and K is the Torrent measurement (10^{-16} m²)

This law (15) could be used to calculate the saturation level from a permeability measurement with knowledge of the carbonation depth from phenolphthalein spraying on the fresh core sampled from the concrete structure.

In view of Figures 10 through 13, standard deviation appears to decrease when saturation level increases (only beyond a saturation level of 15%) to reach the lowest values for samples with an 84% saturation level. However, this observation is surprising since permeability measurements were conducted on completely dry samples, a condition required for correct measurement of the gas permeability. So, the coefficients of variation according to the saturation levels for the four carbonation depths studied are displayed in Figure 14.

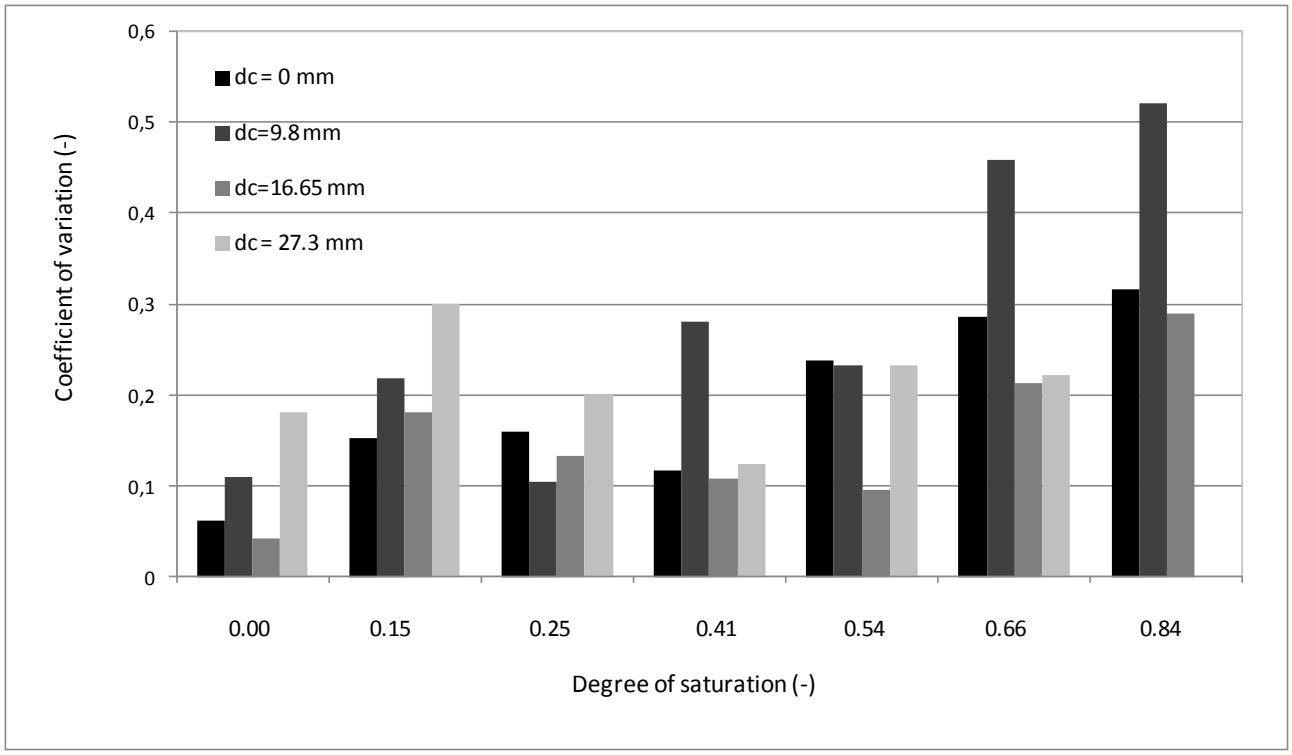

Figure 14: Coefficient of variation of Torrent permeability measurements as a function of saturation degree and carbonation depth.

The results presented in Figure 14 are closer to expectations. Carbonation depth has no effect on the measurements because trends observed in the carbonated slabs differ depending on the saturation level. CoV, on the other hand, effectively increases with the degree of saturation. It should be noted, however, that CoV could not be measured for d_c = 27.3 mm at an 84.1% saturation level, which was at the device operating limit. Moreover, with this saturation level, the coefficient of variation ranges between 30 and 50%. This high range raises questions as to measurement reliability. With these saturation levels, the device operating limits are exceeded, all the more so when the concrete is compact. A key idea of this analysis is that saturation level S and carbonation depth d_c can be determined from the measured K and ρ by combining Equation 15 with Equation 11 or 12. However, these established relationships apply only if the concrete porosity is equivalent (about 18%) and the formulation uses CEM I cement, as in this study. Resistivity and permeability measurements depend on the material composition, which in turn affects the porosity and conductivity of the pore solution.

Moreover, the combination of the two laws is possible only if both measurements can be performed simultaneously, i.e., when the concrete saturation level falls within the range 40-83 %, which is quite often the case where in situ concrete is concerned.

4 Result analysis

4.1 Correlation between resistivity and Torrent gas permeability

Figure 15 shows the correlation between Torrent gas permeability measurements for dried slabs (S= 0%) and resistivity measurements carried out on saturated slabs (S = 100%). This comparison is possible since the saturation level is set aside as the impact of pore saturation is canceled out. The symbols used are the same as in Figures 5 through 8 and 10 through 13. A linear correlation is observed between the two parameters. The slabs with the highest permeability present the lowest resistivity. Both properties share some crucial pore structure characteristics, such as total porosity, pore tortuosity and connectivity, of the cover concrete subjected to carbonation. They are sensitive to the different phases occurring within pores: gas permeability is linked with the characteristics of the gas phase and resistivity depends on the liquid phase through its electrochemical composition. Nevertheless, a good linear correlation is observed for the material studied here. The correlation established by Gui et al. [Gui 2016] for a study conducted to examine gas permeability using the Cembureau device and electrical conductivity using the high frequency alternating current method on laboratory concrete specimens with different water to binder ratios and different admixtures is not as good as the correlation proposed in this paper.

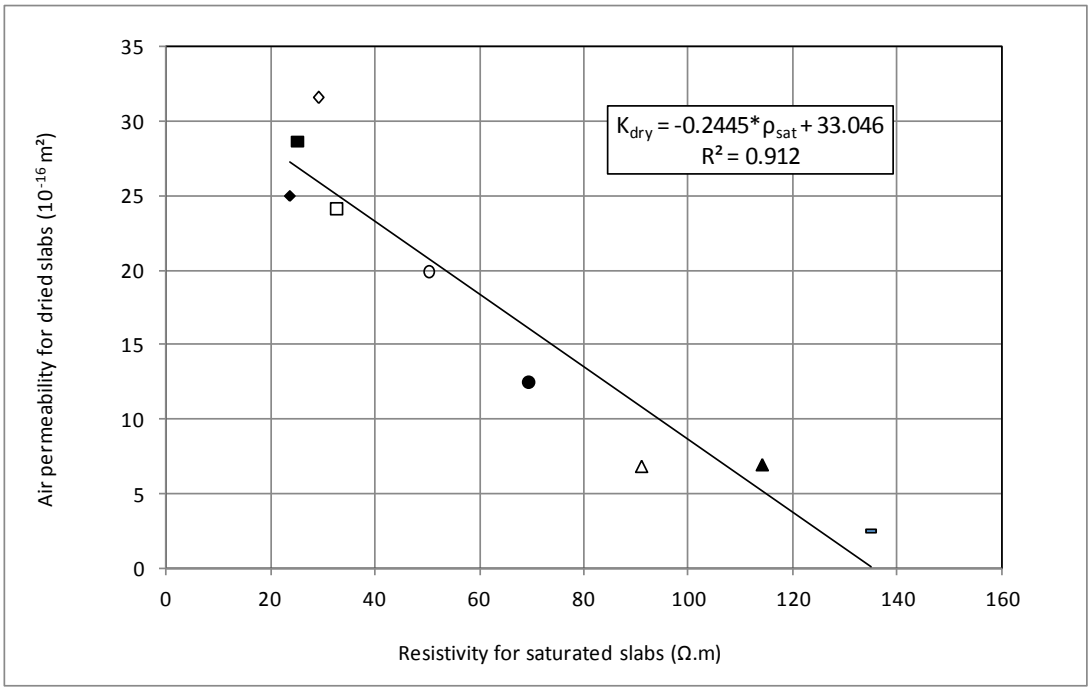

Figure 15: Torrent permeability for dried slabs versus resistivity for saturated slabs

4.2 Resistivity analysis

Relative resistivity is considered because it could be useful to compare different concretes: it has been used by Gui el al. to study electrical conductivity and gas permeability of concrete formulated with CEM I and blast-furnace slag cement [Gui, 2016]. Using a relative value for resistivity and permeability could also be very useful for a modeling approach [Li, 2016]. Resistivity values are then processed after dividing them by the reference value ρ_{ref}. This value can be considered as an intrinsic transport property since the impact of carbonation and pore saturation is canceled out. This value is measured directly on the slabs using the Wenner method. However, in future, taking the value measured on laboratory samples as the reference value when selecting concrete type might be contemplated [Baroghel-Bouny, 2004; Aït-Mokhtar, 2013].

We use the following relationship to fit the experimental data:

$$\frac{\rho}{\rho_{ref}} = A * (1 - S) + B \quad (16)$$

with $A=a/\rho_{ref}$ and $B = b/\rho_{ref}$, a and b being the values reported in Table 6.

549 Solutions are obtained from Equations 8 and 9 as:

550 $$A = 3.317 * \ln(d_c) + 16 \quad (17)$$

551 $$b = 0.1455 * d_c + 1 \quad (18)$$

552 Considering Archie's law, Equation 16 becomes:

553 $$\frac{\rho}{\rho_{ref}} = S^{-n}\phi^{-(m-m_{ref})} \quad (19)$$

554 where n= 2.24, m_{ref} corresponds to the value calculated in Section 3.1, m_{ref} = 3.153, and
555 values of m are given by Equation 10. We have:

556 $$\frac{\rho}{\rho_{ref}} = (3.317 * \ln(d_c) + 16) * (1 - S) + (0.1455 * d_c + 1) \quad (20)$$

557 $$\frac{\rho}{\rho_{ref}} = S^{-n}\phi^{-(m-m_{ref})} \quad (21)$$

558 where $m = 0.0389 * d_c + 3.153$ and d_c is the carbonation depth in mm

559

560 If these laws are validated with concretes presenting other porosities, they may be used for
561 different concrete types if the ρ_{ref} measurement is given. This ρ_{ref} measurement value should
562 become a durability indicator on which the choice between concretes for engineering
563 structures could be based [Baroghel-Bouny, 2004].
564 These laws present equations with two unknown variables (saturation level and carbonation
565 depth) whereas the survey of the structure provides only the resistivity ρ. Consequently, it is
566 essential to combine this equation (linear or exponential) with the relationship established for
567 permeability.

568
569 ### 4.3 Permeability analysis

570 In order to establish correlations that are independent of the permeability measured on dry,
571 non-carbonated concrete, a relative permeability approach is used [Djerbi Tegguer 2013,
572 Kameche 2014]. Permeability values are then processed after being dividing by the reference
573 value $K_{ref,T}$. This value, which is the average value of the Torrent permeability measurements

574 on dry Slabs C1-1-8-N, C1-1-7-N, C1-1-1-T and C1-1-2-T, is 27.34 10-16 m². The
575 permeability measured on a sound, dry sample should become a mandatory parameter for
576 selecting concrete mixtures. This value can be considered as an intrinsic transport property
577 since the impact of carbonation and pore saturation is canceled out. This measurement value
578 might become a durability indicator that could be provided with the formulation of concrete
579 [Baroghel-Bouny 2004, Aït-Mokhtar 2013].
580 The results are displayed in Figures 16 through 19 for different carbonation depths. They are
581 fitted first with a linear law, then with a Van Genuchten law modified by Mualem [1976] and
582 used by [Kameche 2014] to represent relative permeability as a function of saturation level.
583 When fitting with the linear law, the coefficients of determination achieved using Equation 15
584 are obtained as:

585 $$\frac{K}{K_{ref,T}} = e^{-0,0935*d_c} * (1 - S) \quad (22)$$

586 with d_c the carbonation depth in mm.
587 The modified Van Genuchten law (VG law) is then defined as:

588 $$\frac{K}{K_{ref,T}} = (1 - S)^q * (1 - S^2) \quad (23)$$

589 Parameter q is determined by fitting this law with the experimental results obtained on non-
590 carbonated slabs. The results displayed in Figure 16 show that q = 0.89. This value is lower
591 than the values previously achieved for cementitious materials. Monlouis-Bonnaire
592 [Monlouis-Bonnaire 2004] proposes q = 5.5 for cementitious materials and [Kameche 2014],
593 q = 3.5 for relative gas permeabilites measured using the Cembureau method. Permeability
594 variations are very pronounced when they are measured using the Torrent permeameter. For a
595 40% saturation level, relative permeability is 0.6 with the Torrent method but only 0.1 with
596 the Cembureau method [Kameche 2014]. Parameter q, used to quantify the effect of saturation
597 level on relative permeability, is held constant for carbonated slabs. However, a C factor is
598 introduced to consider the decrease in relative permeability with carbonation.

The VG law then becomes:

$$\frac{K}{K_{ref,T}} = C * (1 - S)^q * (1 - S^2) \quad (24)$$

Figure 20 presents the empirical parameter, C, determined by fitting with the experimental results.

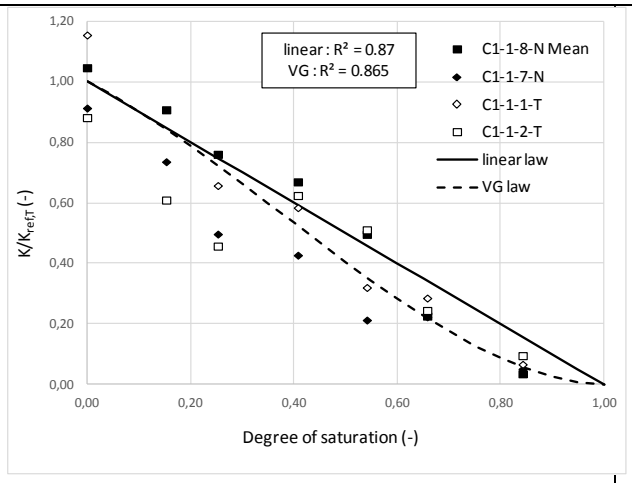

Figure 16: Relative permeability versus saturation degree for non-carbonated slabs

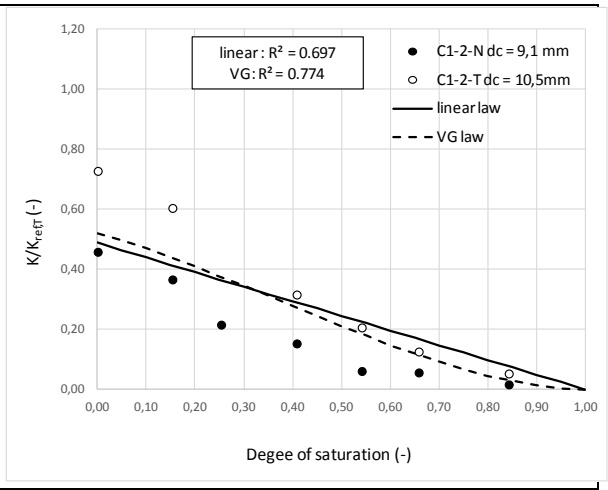

Figure 17: Relative permeability versus saturation degree for carbonated slabs C1-2-N et C1-2-T ($d_{c\ mean}$ = 9.8 mm)

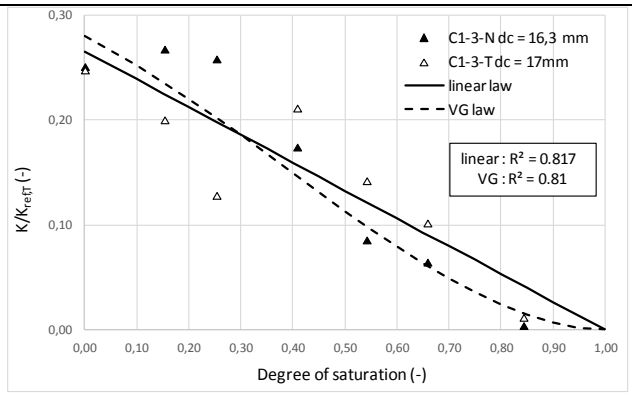

Figure 18: Relative permeability versus saturation degree for carbonated slabs C1-3-N et C1-3-T ($d_{c\ mean}$ = 16.65 mm)

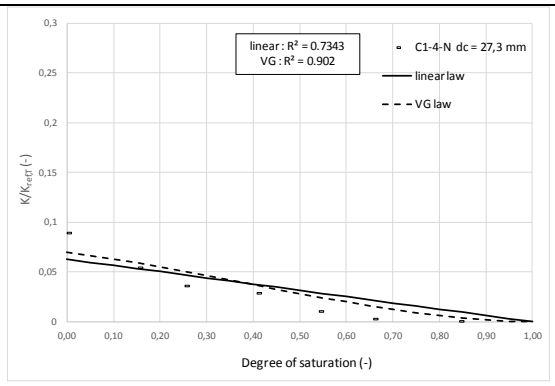

Figure 19 : relative permeability versus saturation degree for carbonated slabs C1-4-N (d_c = 27.3 mm)

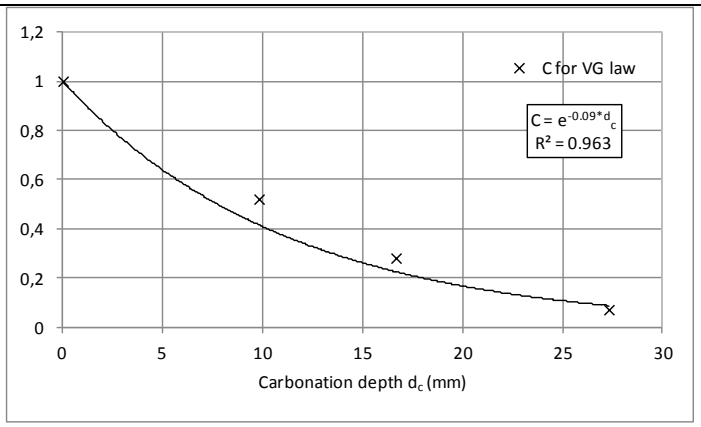

Figure 21: Parameter C of the V.G. law as a function of carbonation depth

The coefficients of determination demonstrate that the VG law describes relative permeability evolution better. This law can therefore be used to describe Torrent permeability evolution according to carbonation depth and saturation level as:

$$\frac{K}{K_{ref,T}} = e^{-0.09*d_c} * (1-S)^{0.89} * (1-S^2) \quad (25)$$

with d_c the carbonation depth in mm.

The VG law for relative permeability and Archie's law for relative resistivity can be used to obtain better coefficients of determination than with linear laws, in particular for carbonated slabs. The two laws can be combined to determine the saturation level and the carbonation depth of similar concrete structures. However, in order to use both measurement techniques simultaneously, the concrete saturation level of the structure must fall within the range 40-66%.

If validated with concrete presenting other porosities, these laws may also be used on other concrete materials if $K_{ref,T}$ measurements, carried out using the Torrent permeameter on dry non-carbonated samples, and ρ_{ref} measurements, carried out using the Wenner resistivimeter on saturated non-carbonated samples, are given. Both measurements could be performed prior to the construction in order to ensure the best choice of concrete formulations. During the survey conducted to apply these laws, the surveyed areas of the structure should be checked

for cracking, as concrete damage modifies permeability [Picandet, 2001; Djerbi, 2008 and 2013] as well as resistivity measurements [Taillet, 2014; Lataste 2003]. If damage is detected, another non-destructive technique should be used and relationships between, for instance, resistivity measurement and saturation level, carbonation depth and damage should be established.

4.4 Validation using a concrete wall

The slabs studied in this paper were used to examine the influence of carbonation on NDT measurements by studying moisture homogeneity on saturated or partially saturated concrete. Equations 11, 12 and 15 were established using experimental measurements carried out on the slabs. In order to validate the performance of these laws, an experimental wall, 100 cm x 75 cm and 20 cm thick, was prepared (Figure 21a). The concrete used for the wall was the same as for the slabs. A reinforcement mesh was placed at a depth of 25 mm on one face of the wall. The diameter of the bars was 10 mm and the size of square mesh was 20 cm. Measurements were only made on the non-reinforced side of the wall in order to avoid the influence of the reinforcement, especially on resistivity measurements. This face of the wall was divided into three vertical sections corresponding to different carbonation depths. After 28 days of storage in a humid chamber, the first section (noted 1 in Figure 21), corresponding to a carbonation depth of 0 mm, was completely sealed. Then, the wall was placed in a carbonation chamber at 20 °C and 65% relative humidity, with a CO2 content of 50% to accelerate the carbonation process. Section 2, corresponding to a carbonation depth of 20 mm, was also sealed after the same exposure to the carbonation process as Slabs C1-3N and C1-3T. The wall was finally removed from the carbonation chamber after the same exposure time as Slab C1-4N.

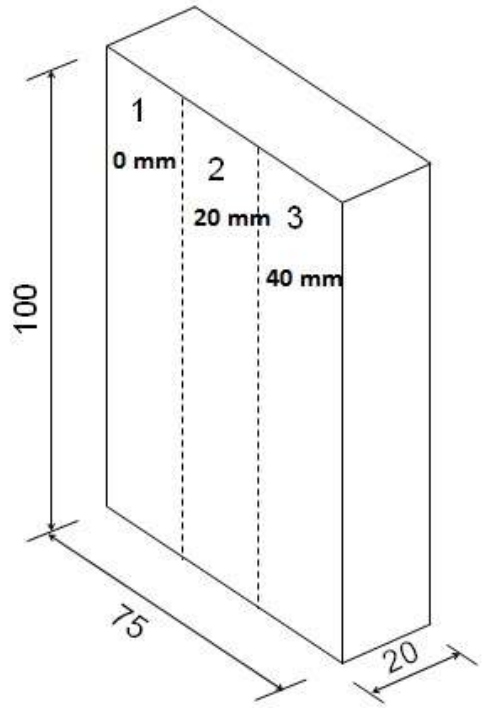

a) Wall dimensions

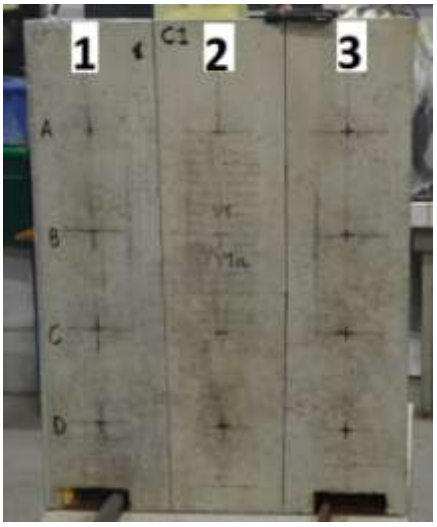

b) Photo of the wall

Figure 21: Experimental concrete wall

NDT measurements were carried out at twelve points on the wall (indicated with crosses in Figure 21b). Then, core samples were taken in the center of each mesh to obtain real carbonation depths and saturation levels. Each core sample was cut into three pieces: one from each end, with a thickness corresponding to the desired carbonated depth, and one middle piece corresponding to sound concrete (non-carbonated). Because coring and sawing were done under water, at the end of the operations, samples were dried with a cloth to avoid the absorption of water as far as possible and so to avoid modifying the moisture content. The carbonation depth was observed by spraying the core samples with the phenolphthalein color indicator and the saturation level was calculated after drying the core samples as described in Section 2.3. The values reported in Table 7 are the mean values obtained from 8

660 measurements (four core samples for each vertical section and two pieces for each core
661 sample).

Vertical section	Measured carbonation depth (mm)	Measured saturation level (%)	Mean permeability 10^{-16} m²	Mean Wenner resistivity Ω.m	Calculated carbonation depth (mm)		Calculated saturation level (%)	
					equations 11 + 15	**equations 12 + 15**	**equations 11 + 15**	**equations 12 + 15**
1	0.25	65	1.7	22	0.003	0	93.7	93.7
2	18.9	58.9	1.07	407	24.4	24.38	61.7	61.8
3	33.1	60.6	0.101	504	48.8	38.9	64.9	86

662 *Table 7: Comparison between measured and calculated values of carbonation depth and*
663 *saturation level.*
664
665 In Section 1, Torrent permeability measurements were carried out with a saturation level that
666 was considered high for such a measuring technique. As shown in Figure 14, CoV increased
667 with the degree of saturation. This can explain the high calculated degree of saturation
668 obtained in Section 1 in both cases (Equations 11+15 and 12+15). As regards the carbonated
669 sections, the calculated values for carbonation depth were overestimated by non-destructive
670 testing, which provides a safety margin regarding the service life assessment of concrete
671 structures but can be expensive for owners because repair will take place earlier. The
672 combination of Equations 12 and 15 is more consistent with the measured data especially as
673 regards carbonation depth. This combination is recommended for carbonation depth
674 calculations, while the combination of Equations 11 and 15 is advised for calculating the
675 saturation level after testing concrete structures using the Wenner resistivimeter and the
676 Torrent permeameter.
677
678 ## 5 Conclusion
679 In this study, resistivity and permeability measurements were performed on carbonated slabs
680 conditioned at different saturation degrees. The results confirm that resistivity and
681 permeability are both very sensitive to concrete moisture. They also clearly show that

carbonation affects resistivity and permeability. The higher the carbonated depth is, the higher is the resistivity and the lower is the permeability. This can be related to the reaction of carbonation, which decreases porosity. Resistivity cannot be assessed for water saturation degrees of less than 40% because, at such low moisture content, the continuity of the interstitial solution vanishes and the electrical current cannot circulate. On the other hand, permeability cannot be measured for saturation degrees higher than 83% due to the obstruction of pores by the interstitial solution, which prevents gas penetration. An analysis of the test results has shown a coefficient of variation of 20% for resistivity and less than 30% for permeability, which increases with the increase of saturation degree whatever the carbonated depth.

Two empirical laws have been proposed here to model resistivity measurements versus carbonated depth and saturation degree. The first one is adapted from a linear law between resistivity and saturation degree to take the carbonated depth into account. For the second one, Archie's law is adapted to take carbonation into account. The coefficient of determination is better for the linear model, which is easier to determine. In the same way, a linear model between permeability coefficient and saturation degree is extended to take the carbonated depth into account with a good determination coefficient.

Models involving relative resistivity and relative permeability have also been proposed. For resistivity, both the linear and Archie's law are considered. For permeability modeling, a modified Van Genuchten law seems more efficient than the modified linear model. It would be interesting to check these models with concrete presenting other porosities.

Finally, the different models have been used to predict both saturation degree and carbonated depth on a wall made with the same concrete as the slabs. The results show that the models are able to distinguish different carbonated depths but the assessment precision needs to be improved. Additional research is required, in particular to take the presence of cracks into

consideration. These may due to shrinkage or to mechanical effects, for instance, which have a significant influence on measurements. In order to improve the quality of the investigation, a third technique could be proposed, such as ultrasonic surface waves, which are able to investigate the cover concrete.

6 Acknowledgment

The French National Research Agency (ANR "Building and Sustainable Cities") is gratefully acknowledged for supporting the ANR EvaDéOS project. Our thanks are extended to Susan Becker, a native English speaker, commissioned to proofread the final English version of this paper.

7 References

[Aït-Mokhtar 2013] Aït-Mokhtar A., Belarbi R., Benboudjema F., Burlion N., Capra B., Carcassès M., Colliat J.-B., Cussigh F., Deby F., Jacquemot F., De Larrard T., Lataste J.-F., Le Bescop P., Pierre M., Poyet S., Rougeau P., Rougelot T., Sellier A., Séménadisse J., Torrenti J.-M., Trabelsi A., Turcry P., Yanez-Godoy H., Experimental investigation of the variability of concrete durability properties, Cement and Concrete Research 45 (2013) 21–36.

[Abbas 1999] Abbas A., Carcasses M., Ollivier J.P., Gas permeability of concrete in relation to its degree of saturation, Materials and Structures, Vol. 32, January-February 1999, pp 3-8.

[Andersson 1989] Andersson K., Allard B , Bengtsson M., Magnusson B., chemical composition of cement pore solutions, cement and concrete research, Vol. 19, pp. 327-332, 1989.

[Archie 1942] Archie G.E., The electrical resistivity log as an aid in determining some reservoir characteristics, Transaction of AIME, 1942, 146, pp.54-62

[Baroghel-Bouny 2004] Baroghel-Bouny, V., "Concrete design for structures with predefined service life – durability control with respect to reinforcement corrosion and alkali–silica reaction state-of-the-art and guide for the implementation of a performance-type and predictive approach based upon durability indicators." English version of Documents Scientifiques et Techniques de l'AFGC (Civil Engineering French Association), 2004.

[Bungey 2006] Bungey J., Millard S., Grantham M., Testing of Concrete in Structures, 4th Edition, Taylor and Francis Editors, 2006.

[Auroy 2015] Auroy M., Poyet S., Le Bescop P., Torrenti J.M., Charpentier T., Moskura M., Bourbon X., Impact of carbonation on unsaturated water transport properties of cement-based materials, Cement and Concrete Research, Volume 74, August 2015, Pages 44-58.

[Breysse 2017] D. Breysse, J.-P. Balayssac, S. Biondi, A. Borosnyói, E. Candigliota, L. Chiauzzi, V. Garnier, M. Grantham, O. Gunes, V. Luprano, A. Masi, V. Pfister, Z.M. Sbartai, K. Szilagyi, M. Fontan, Non Destructive Assessment of In-situ Concrete Strength: comparison of approaches through an international benchmark, Materials and Structures, Vol. 50, N°133, 2017

[Chang 2004] Chang J.J., Yeih W., Huang R., Chen C.T., Suitability of several current used concrete durability indices on evaluating the corrosion hazard for carbonated concrete, Mater. Chem. Phys., vol. 84, n° 1, p. 71‑78, March 2004.

[Chang 2006] Chang C.F., Chen J.W., The experimental investigation of concrete carbonation depth, Cement and Concrete Research 36 (2006) 1760– 1767.

[Djerbi 2008] Djerbi A., Bonnet S., Khelidj A., Baroghel-Bouny V., Influence of traversing crack on chloride diffusion into concrete, Cement and Concrete Research 38 (2008) 877–883.

[Djerbi Tegguer 2013] Djerbi Tegguer A., A., Bonnet S., Khelidj A., Baroghel-Bouny V., Effect of uniaxial compressive loading on gas permeability and chloride diffusion coefficient of concrete and their relationship, Cement and Concrete Research 52 (2013) 131–139.

[Du Ploy 2015] Du Plooy R., Villain G., Palma Lopes S., Ihamouten A., Dérobert X., Thauvin B., Electromagnetic non-destructive evaluation techniques for the monitoring of water and chloride ingress into concrete: a comparative study, Materials and structures 48 (2015) 369-386.

[Fares 2018] Fares M., Villain G., Bonnet S., Palma Lopes S., Thauvin B., Thiery M., Determining chloride content profiles in concrete using a resistivity probe, submitted to Cement and concrete Composites in September 2017.

[Gui 2016] Gui Q., Qin M., Li K., Gas permeability and electrical conductivity of structural concretes: Impact of pore structure and pore saturation, Cement and Concrete Research 89 (2016) 109–119.

[Houst 1983] Houst Y.F., Roelfstra P. E., Wittmann F.H., A model to predict service life of concrete structures, *Mater. Sci. Restor.*, p. 181‑186, 1983.

[Hui-Sheng 2009] Hui-Sheng S., Bi-Wan X., Xiao-Chen Z., Influence of mineral admixtures on compressive strength, gas permeability and carbonation of high performance concrete, Construction and Building Materials 23 (2009) 1980-1985.

[Kameche 2014] Kameche Z.A., Ghomari F., Choinska M., Khelidj A., Assessment of liquid water and gas permeabilities of partially saturated ordinary concrete, Construction and Building Materials 65 (2014) 551–565.

[Lataste 2003] Lataste J.F., Sirieix C., Breysse D., Frappa M., Electrical resistivity measurement applied to cracking assessment on reinforced concrete structures in civil engineering, NDT & E International, Volume 36, Issue 6, September 2003, Pages 383-394

[Lecieux 2015] Lecieux Y., Schoefs F., Bonnet S., Lecieux T., Lopes S.P., Quantification and uncertainty analysis of a structural monitoring device: detection of chloride in concrete using DC electrical resistivity measurement, Nondestructive Testing and Evaluation 30(3) (2015) 216-232.

[Li 2016] Li K., Stroeven M., Stroeven S., Sluys L.J., Investigation of liquid water and gas permeability of partially saturated cement paste by DEM approach, Cement and Concrete Research 83 (2016) 104–113.

[Lopez 1993] Lopez W., Gonzalez J.A., Influence of the degree of pore saturation on the resistivity of concrete and the corrosion of steel reinforcement, Cement and Concrete Research. Vol. 23 (1993) 368-376.

[Lübeck 2012] Lübeck A., Gastaldini A.L.G. , Barin D.S., Siqueira H.C., Compressive strength and electrical properties of concrete with white Portland cement and blast-furnace slag, Cement and Concrete Composites, Volume 34, Issue 3, March 2012, Pages 392–399.

[Monlouis-Bonnaire 2004] Monlouis-Bonnaire JP, Verdier J, Perrin B. Prediction of the relative permeability to gas flow of cement-based materials. Cem Concr Res 2004; 34:737–44.

[Mualem 1976] Mualem Y A new model for predicting the unsaturated hydraulic conductivity of porous media Water Resour Res 1976;12:513–22.

[Neithalath 2006] Neithalath N., Weiss J., Olek J., Characterizing Enhanced Porosity Concrete using electrical impedance to predict acoustic and hydraulic performance, Cement and Concrete Research 36 (2006), 2074–2085.

[Neves 2012] Neves R., Branco F., De Brito J., About the statistical interpretation of air permeability assessment results, Materials and Structures 45 (2012) 529–539.

[Neves 2015] Neves R., Sena Da Fonseca B., Branco F., Brito J., Castela A., Montemor M.F., Assessing concrete carbonation resistance through air permeability measurements, Construction and Building Materials 82 (2015) 304-309

[Ngala 1997] Ngala V.T., Page C.L., Effects of carbonation on pore structure and diffusional properties of hydrated cement pastes, Cem. Concr. Res. 27 (1997) 995–1007.

[Nguyen 2006] Nguyen T.S., Influence of binder and temperature on the chloride transport in cemntious materials, PhD thesis, LMDC Toulouse France, (September 2006), in French.

[Nguyen 2017] Estimation of reinforcement electrochemical state in water-saturated reinforced concrete by resistivity measurement, Construction and Building Materials, Vol. 171, May 2018, Pages 455-466

[Papadakis 1989] Papadakis V.G. , A reaction engineering approach to the problem of concrete carbonation, *AIChE J.*, vol. 35, n° 10, p. 1639–1650, 1989.

[Papadakis 1999] Papadakis V.G., Effect of fly ash on Portland cement systems: Part I. Low-calcium fly ash, *Cem. Concr. Res.*, vol. 29, n° 11, p. 1727–1736, 1999.

[Papadakis 2000] Papadakis V.G., Effect of fly ash on Portland cement systems: Part II. High-calcium fly ash, *Cem. Concr. Res.*, vol. 30, n° 10, p. 1647–1654, 2000.

[Picandet 2001] Picandet V., Khelidj A., Bastian G., Effect of axial compressive damage on gas permeability of ordinary and high-performance concrete, Cement and Concrete Research 31 (2001) 1525–1532.

[Polder 2001] Polder R., Test methods for on site measurement of resistivity of concrete – a RILEM TC-154 Technical Recommendation, Construction Building Materials 15 (2001) pp. 125–31.

[RILEM CPC-18] RILEM CPC-18, RILEM Committee, Measurement of hardened concrete carbonation depth, Mater. Struct. 18 (1988) 453–455.

[Romer 2005] Romer M., Effect of moisture and concrete composition on the Torrent permeability measurement, Materials and Structures 38 (June 2005) 541-547.

827 [Saetta 1993] Saetta A.V., The carbonation of concrete and the mechanism of moisture, heat
828 and carbon dioxide flow through porous materials, *Cem. Concr. Res.*, vol. 23, p. 761-772,
829 1993.

830 [Saleem 1996] Saleem M., Shameemt M., Hussain S.E., Maslehuddintf M., Effect of
831 moisture, chloride and sulphate contamination on the electrical resistivity of Portland cement
832 concrete, Construction and Building Materials, Vol. 10, No. 3, (1996) 209-214.

833 [Sanish 2013] Sanish K.B., Neithalath N., Santhanam M., Monitoring the evolution of
834 material structure in cement pastes and concretes using electrical property measurements,
835 Construction and Building Materials, Volume 49, December 2013, Pages 288-297

836 [Sant 2011] Sant G., Bentz D., Weiss J., Capillary porosity depercolation in cement-based
837 materials: Measurement techniques and factors which influence their interpretation, Cement
838 and Concrete Research 41 (2011) 854–864.

839 [Sena da Fonseca 2015] Sena da Fonseca B., Castela A.S., Duarte R.G., Neves R., Montemor
840 M. F., Non-destructive and on site method to assess the air- permeability in dimension stones
841 and its relationship with other transport-related properties, Materials and Structures (2015) vol
842 48, 3795–3809, DOI 10.1617/s11527-014-0440-2

843 [Sbartaï 2007] Sbartaï Z.M., Laurens S., Rhazi J., Balayssac J.P., Arliguie G., Using radar
844 direct wave for concrete condition assessment: Correlation with electrical resistivity, Journal
845 of Applied Geophysics 62 (2007) 361–374

846 [Shi 2004] Shi C., Effect of mixing proportions of concrete on its electrical conductivity and
847 the rapid chloride permeability test (ASTM C1202 or ASSHTO T277) results, Cement and
848 Concrete Research 34, pp 537–545, 2004.

849 [Ta 2016] Ta V.L, Bonnet S., Senga Kiesse T., Ventura A., A new meta-model to calculate
850 carbonation front depth within concrete structures, Construction and Building Materials 129
851 (2016) 172–181

852 [Ta 2018] Ta V. L., Senga Kiesse T., Bonnet S., Ventura A., Application of sensitivity
853 analysis in the life cycle design for the durability of reinforced concrete structures in the case
854 of XC4 exposure class, Cement and Concrete Composites, Volume 87, 2018, Pages 53–62,
855 https://doi.org/10.1016/j.cemconcomp.2017.11.024.

856 [Taillet 2014] Taillet E., Lataste J.F., Rivard P., Denis A., Non-destructive evaluation of
857 cracks in massive concrete using normal dc resistivity, NDT & E International, Volume 63,
858 April 2014, Pages 11-20

859 [Torrent 1992] Torrent R.J., A two-chamber vacuum cell for measuring the coefficient of
860 permeability to air of the concrete cover on site, Materials and Structures 25 (1992) 358-365.

861 [Villain 2001] Villain G., Baroghel-Bouny V. Hua C., Measuring the gas permeability as a
862 function of saturation rate of concretes, French J Civ Eng 2001, [Transfer in concrete and
863 durability, In French].

864 [Villain 2006] Villain G., Thiery M., Gammadensimetry: A method to determine drying and
865 carbonation profiles in concrete, NDT&E International 39 (2006) 328–337.

866 [Younsi 2011] Younsi A., Turcry P., Rozière E., Aït-Mokhtar K., Loukili A., Performance-
867 based design and carbonation of concrete with high fly ash content, *Cem. Concr. Compos.*,
868 vol. 33, n° 10, p. 993-1000, nov. 2011.

869 [Zhou 2001] Zhou Q., F.P. Glasser F.P., Thermal stability and decomposition mechanisms of
870 ettringite at <120°C, Cement and Concrete Research, vol. 31 (2001) 1333–1339.